Measurement of Structure-Dependent $K^+ \to \mu^+ \nu_\mu \gamma$ Decay

S. Adler,[1] M. S. Atiya,[1] I-H. Chiang,[1] M. V. Diwan,[1] J. S. Frank,[1] J. S. Haggerty,[1] S. H. Kettell,[1] T. F. Kycia,[1,*] K. K. Li,[1] L. S. Littenberg,[1] A. Sambamurti,[1,*] A. Stevens,[1] R. C. Strand,[1] C. Witzig,[1] T. K. Komatsubara,[2] M. Kuriki,[2] N. Muramatsu,[2] S. Sugimoto,[2] T. Inagaki,[3] S. Kabe,[3] M. Kobayashi,[3] Y. Kuno,[3] T. Sato,[3] T. Shinkawa,[3] Y. Yoshimura,[3] Y. Kishi,[4] T. Nakano,[4] M. Ardebili,[5] M. R. Convery,[5] M. M. Ito,[5] D. R. Marlow,[5] R. A. McPherson,[5] P. D. Meyers,[5] F. C. Shoemaker,[5] A. J. S. Smith,[5] J. R. Stone,[5] M. Aoki,[6,†] E. W. Blackmore,[6] P. C. Bergbusch,[6,8] D. A. Bryman,[6,8] A. Konaka,[6] J. A. Macdonald,[6] J. Mildenberger,[6] T. Numao,[6] P. Padley,[6] J.-M. Poutissou,[6] R. Poutissou,[6] G. Redlinger,[6,‡] P. Kitching,[7] and R. Soluk[7]

(E787 Collaboration)

[1]*Brookhaven National Laboratory, Upton, New York 11973*
[2]*High Energy Accelerator Research Organization (KEK), Tanashi-branch, Midoricho, Tanashi, Tokyo 188-8501, Japan*
[3]*High Energy Accelerator Research Organization (KEK), Oho, Tsukuba, Ibaraki 305-0801, Japan*
[4]*RCNP, Osaka University, 10-1 Mihogasaki, Ibaraki, Osaka 567-0047, Japan*
[5]*Joseph Henry Laboratories, Princeton University, Princeton, New Jersey 08544*
[6]*TRIUMF, 4004 Wesbrook Mall, Vancouver, British Columbia, Canada V6T 2A3*
[7]*Centre for Subatomic Research, University of Alberta, Edmonton, Alberta, Canada T6G 2N5*
[8]*Department of Physics and Astronomy, University of British Columbia, Vancouver, British Columbia, Canada V6T 1Z1*

(Received 17 March 2000)

We report the first measurement of a structure-dependent component in the decay $K^+ \to \mu^+ \nu_\mu \gamma$. Using the kinematic region where the muon kinetic energy is greater than 137 MeV and the photon energy is greater than 90 MeV, we find that the absolute value of the sum of the vector and axial-vector form factors is $|F_V + F_A| = 0.165 \pm 0.007 \pm 0.011$. This corresponds to a branching ratio of $B(\mathrm{SD}^+) = (1.33 \pm 0.12 \pm 0.18) \times 10^{-5}$. We also set the limit $-0.04 < F_V - F_A < 0.24$ at 90% C.L.

PACS numbers: 13.20.Eb, 13.40.Ks

The decay $K^+ \to \mu^+ \nu_\mu \gamma$ ($K_{\mu\nu\gamma}$) can proceed via two distinct mechanisms. The first, internal bremsstrahlung (IB), is a radiative version of the familiar $K^+ \to \mu^+ \nu_\mu$ ($K_{\mu 2}$) decay: its Feynman diagram has a photon emitted from the external kaon or muon line. The second, structure-dependent radiative decay (SD), involves the emission of a photon from intermediate states. SD is sensitive to the electroweak structure of the kaon and has been the subject of an extensive theoretical literature [1,2]. In recent years most of this has been in the framework of chiral perturbation theory (ChPT) [3]. The differential rate in the K^+ rest frame can be written [2] in terms of $x \equiv \frac{2E_\gamma}{M_K}$ and $y \equiv \frac{2(E_\mu + M_\mu)}{M_K}$, where E_γ is the photon energy, E_μ is the muon kinetic energy, M_μ is the μ^+ mass, and M_K is the K^+ mass:

$$\frac{d\Gamma_{K_{\mu\nu\gamma}}}{dxdy} = A_{\mathrm{IB}} f_{\mathrm{IB}}(x,y) + A_{\mathrm{SD}}[(F_V + F_A)^2 f_{\mathrm{SD}^+}(x,y) + (F_V - F_A)^2 f_{\mathrm{SD}^-}(x,y)] - A_{\mathrm{INT}}[(F_V + F_A) f_{\mathrm{INT}^+}(x,y) + (F_V - F_A) f_{\mathrm{INT}^-}(x,y)], \quad (1)$$

$$f_{\mathrm{IB}}(x,y) = \left[\frac{1 - y + r}{x^2(x + y - 1 - r)}\right]\left[x^2 + 2(1 - x)(1 - r) - \frac{2xr(1 - r)}{x + y - 1 - r}\right], \quad (2)$$

$$f_{\mathrm{SD}^+} = [x + y - 1 - r][(x + y - 1)(1 - x) - r], \quad (3)$$

$$f_{\mathrm{SD}^-} = [1 - y + r][(1 - x)(1 - y) + r], \quad (4)$$

$$f_{\mathrm{INT}^+} = \left[\frac{1 - y + r}{x(x + y - 1 - r)}\right] \times [(1 - x)(1 - x - y) + r], \quad (5)$$

$$f_{\mathrm{INT}^-} = \left[\frac{1 - y + r}{x(x + y - 1 - r)}\right] \times [x^2 - (1 - x)(1 - x - y) - r], \quad (6)$$

$$r = \left[\frac{M_\mu}{M_K}\right]^2, \qquad A_{\mathrm{IB}} = \Gamma_{K_{\mu 2}} \frac{\alpha}{2\pi} \frac{1}{(1 - r)^2}, \quad (7)$$

$$A_{\mathrm{SD}} = \Gamma_{K_{\mu 2}} \frac{\alpha}{8\pi} \frac{1}{r(1 - r)^2} \left[\frac{M_K}{F_K}\right]^2, \quad (8)$$

 0031-9007/00/85(11)/2256(4)$15.00

$$A_{\mathrm{INT}} = \Gamma_{K_{\mu 2}} \frac{\alpha}{2\pi} \frac{1}{(1-r)^2} \frac{M_K}{F_K}. \quad (9)$$

In these formulas, F_V is the vector form factor, F_A is the axial form factor [4], α is the fine structure constant (1/137.036), F_K is the K^+ decay constant (159.8 $\pm$ 1.4 $\pm$ 0.4 MeV), and $\Gamma_{K_{\mu 2}}$ is the width of the $K_{\mu 2}$ decay.

SD^+ and SD^- refer to different photon polarizations, and these components do not mutually interfere. Both SD^+ and SD^- can interfere with IB, however, resulting in the terms labeled INT^+ and INT^-. Figure 1 shows the shapes of f_{IB}, f_{SD^+}, f_{INT^+}, and f_{INT^-}. This analysis is mostly aimed at observing the SD^+ component, which, since it peaks at high muon and photon energy, is the easiest of the SD components to observe. The form factors of the decay, F_V and F_A, can, in principle, depend on q^2, which is given by $q^2 = M_K^2 - 2M_K E_\gamma$ in the K^+ rest frame. In an $\mathcal{O}(p^4)$ ChPT calculation [3,6], however, they are found to be q^2 independent and are given by $F_V + F_A = 0.137$, $F_V - F_A = 0.052$, which corresponds to $B(\mathrm{SD}^+) = 9.22 \times 10^{-6}$. In the data analysis, we initially assume that they are constant, then test for q^2 dependence.

The IB component of $K_{\mu\nu\gamma}$ has been well measured in other experiments and found to agree with the QED prediction [7]. The structure-dependent components, on the other hand, have not yet been measured. For the SD^+ component, the best limit is $B(\mathrm{SD}^+) < 3.0 \times 10^{-5}$ [7]. There is also a limit on the combination $B(\mathrm{SD}^- + \mathrm{INT}^-) < 1.3 \times 10^{-3}$) [7]. In terms of the form factors, these limits translate into $|F_V + F_A| < 0.23$, $-0.3 < (F_V - F_A) < 2.5$.

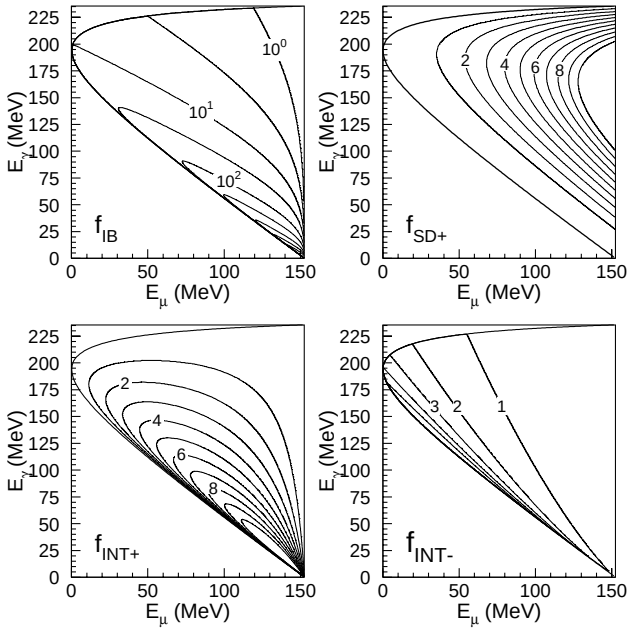

FIG. 1. Dalitz plots for IB, SD^+, INT^+, and INT^- components of $K_{\mu\nu\gamma}$. The normalizations are arbitrary, and the scale on the f_{IB} plot is logarithmic. The SD^- component is not shown because it peaks at low muon momentum and has negligible effect on the current analysis.

In $\mathcal{O}(p^4)$ ChPT, F_V and F_A for the closely related process $K^+ \to e^+ \nu\gamma$ ($K_{e\nu\gamma}$) are identical to those for $K_{\mu\nu\gamma}$. However, in $K_{e\nu\gamma}$ it is possible to measure only the absolute values of the form factors. The $K_{e\nu\gamma}$ experiments [8] give $|F_V + F_A| = 0.148 \pm 0.010$, $|F_V - F_A| < 0.49$, in agreement with $\mathcal{O}(p^4)$ ChPT.

In $K_{\mu\nu\gamma}$, the IB term is large, thus complicating the extraction of the SD terms, but also making the INT terms comparable in size to the SD terms. This makes it possible, in principle, to measure the sign as well as the magnitude of the form factors. In addition to its potential for checking the predictions of ChPT, $K_{\mu\nu\gamma}$ is also interesting as a probe of nonstandard model CP violation [9]. One can look for a T violating component of muon polarization transverse to the plane of the decay. Such an effect is proportional to the INT components.

The E787 experiment at the Brookhaven Alternating Gradient Synchrotron (AGS) [10] was used to look for the SD^+ component. E787, originally designed to search for $K^+ \to \pi^+ \nu\overline{\nu}$, uses a beam of K^+ mesons brought to a stop in a scintillating fiber target. From there, charged decay products can enter the drift chamber where their momentum is measured in a 1-T magnetic field. The charged tracks then enter the range stack (RS), which consists of 21 layers of scintillator and two layers of straw tube chambers (RSSC). Most tracks range out in the RS, thus allowing measurements of their total energy and range. A 4π photon detection system, composed of the barrel veto (BV) and two end caps, surrounds the central region. In the present application the BV, covering 70% of the solid angle and composed of lead and scintillator, is used to detect the photons of interest as well as to rule out the presence of more than one photon.

The $K_{\mu\nu\gamma}$ data were taken with the upgraded E787 detector, which was completed in 1994. In this analysis, the redundant charged track energy and momentum measurements are combined (assuming a μ^+ mass) to give an improved measurement of the track kinematics. The rms resolution of this combined quantity is $\sigma_{p_\mu} = 0.0164 p_\mu - 0.86$ MeV/c, for $205 < p_\mu < 236$ MeV/c, where p_μ is the combined measurement expressed as a momentum. The resolutions for the azimuthal (ϕ) and polar (θ, with respect to the beam) angles of the muons are each 32 mrad. The resolutions on the photon kinematic quantities are $\sigma_{E_\gamma} = 1.676\sqrt{E_\gamma}$ MeV (E_γ in MeV), $\sigma_\phi = 25$ mrad, and $\sigma_\theta = 45$ mrad.

A special trigger designed to search for the SD^+ component of $K_{\mu\nu\gamma}$ required a high energy charged track in the central region, a high energy photon in the BV, and no other photons in the event. A two-day run using this trigger netted a total exposure of 9.2×10^9 K^+, yielding a total of 1.5×10^6 $K_{\mu\nu\gamma}$ triggers.

Analysis of the events passing the trigger proceeds in three steps: event reconstruction, background rejection, and $K_{\mu\nu\gamma}$ spectrum fitting. In the reconstruction step, the energy, time, and flight direction of the charged track and photon are calculated. Any additional photon energy

not associated with the primary photon is also recorded. A kinematic fit to the $K_{\mu\nu\gamma}$ hypothesis is applied to the charged track and the photon. Since there are four constraints (conservation of momentum and energy) and three unmeasured quantities (momentum of the neutrino), the kinematics are overconstrained and non-$K_{\mu\nu\gamma}$ events should have a bad fit χ^2. Additionally, the kinematic fit yields measurements of E_μ and E_γ with better resolution than the raw quantities. These are the variables that are used in the final Dalitz plot fit.

The two main types of background that need to be rejected are $K_{\mu 2}$ accompanied by an accidental photon and $K^+ \to \pi^0\mu^+\nu_\mu$ ($K_{\mu 3}$) or $K^+ \to \pi^+\pi^0$ ($K_{\pi 2}$) where one of the photons from the π^0 decay satisfies the photon requirement and the other photon is undetected. The $K_{\mu 2}$ + accidental background can be suppressed in two independent ways: by requiring a tight time coincidence between the muon and the photon and by examining the kinematics of the decay. Since the accidental photon is randomly oriented relative to the muon, the cut on the χ^2 of the kinematic fit to the $K_{\mu\nu\gamma}$ hypothesis is especially effective against this background. Both $K_{\mu 3}$ and $K_{\pi 2}$ backgrounds can also be rejected in two independent ways: vetoing on any additional photon energy in the event and by the kinematics of the decay. The requirement that the charged track energy be above the $K_{\mu 3}$ end point ($E_{\mu^+} > 137$ MeV) is especially effective against this type of background.

In the final signal region defined by $E_{\mu^+} > 137$ MeV and $E_\gamma > 90$ MeV, the expected background (with statistical error) from the $K_{\mu 2}$ + accidental source is 79.4 ± 4.8 events. The $K_{\mu 3}$ and $K_{\pi 2}$ backgrounds are treated together and give a total expected background of 25.2 ± 3.8 events.

Figure 2(a) shows the final Dalitz plot of events with the final signal region in the upper right corner delineated by the solid line. The number of events in this region is 2693, the vast majority of which are $K_{\mu\nu\gamma}$. As a simple way of testing whether the $K_{\mu\nu\gamma}$ events are consistent with being only IB, we examine the distribution of the opening angle between the muon and the photon ($\cos\theta_{\mu\gamma}$). Figure 2(b) shows this distribution for background-subtracted data. Superimposed on the data are Monte Carlo distributions for IB and SD^+ components of $K_{\mu\nu\gamma}$. When only an IB component is allowed, the quality of the fit is very poor ($\chi^2 = 300$, with 48 degrees of freedom). When an SD^+ contribution is allowed, a much better fit is obtained ($\chi^2 = 58$) [11], clearly indicating that a structure dependent component is present.

The fit is incomplete, however, because it does not include the effects of the other $K^+ \to \mu^+\nu_\mu\gamma$ components (SD^-, INT^+, INT^-). To include these effects, we generate Monte Carlo distributions with SD and INT components weighted by the form factors and normalized to the IB component. In Fig. 3, we plot the χ^2 between the E_{μ^+} vs E_γ histogram of this Monte Carlo sample and that observed in data (after background subtraction)

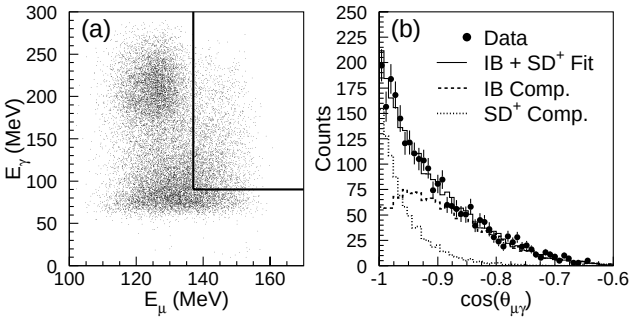

FIG. 2. (a) Dalitz plot of events passing all but the final kinematic cut. Variables plotted are E_μ, the muon kinetic energy, and E_γ, the photon energy. Background from $K_{\mu 3}$ and $K_{\pi 2}$ is concentrated in the region $E_\mu < 137$ MeV and $E_\gamma > 150$ MeV. The IB component of $K_{\mu\nu\gamma}$ is concentrated at $E_\gamma < 100$ MeV. The box marks the final cut of $E_\mu > 137$ MeV and $E_\gamma > 90$ MeV, within which the SD^+ component is enhanced. (b) Counts vs $\cos(\theta_{\mu\gamma})$ and various fits as described in text.

as a function of the form factors. The histogram bins are 3 MeV wide in E_μ and 15 MeV wide in E_γ. The minimum χ^2 is 75 with 69 degrees of freedom. The best fit values are $|F_V + F_A| = 0.165 \pm 0.007$, $F_V - F_A = 0.102 \pm 0.073$, where the errors are statistical. The minimum χ^2's found in the regions where $F_V + F_A < 0$ and where $F_V + F_A > 0$ differ by only 0.2. We thus have no information about the sign of $F_V + F_A$ and can measure only its absolute value. The result corresponds to a branching ratio of $B(SD^+) = (1.33 \pm 0.12) \times 10^{-5}$.

The largest systematic errors associated with the form factor measurements come from possible distortions of the $K_{\mu\nu\gamma}$ spectrum induced by differences between the true detector and the Monte Carlo simulation. The two largest sources of distortion are nonlinearity in the measurement of the photon energy and uncertainty in the thickness of the individual RS scintillator layers. For $|F_V + F_A|$, these two sources lead to uncertainties of 0.0095 and 0.0054, respectively. For $|F_V - F_A|$, they are 0.028 and 0.033. The systematic errors due to uncertainty in the level of background present in the final sample are estimated in data-based background studies. They are found to be very small,

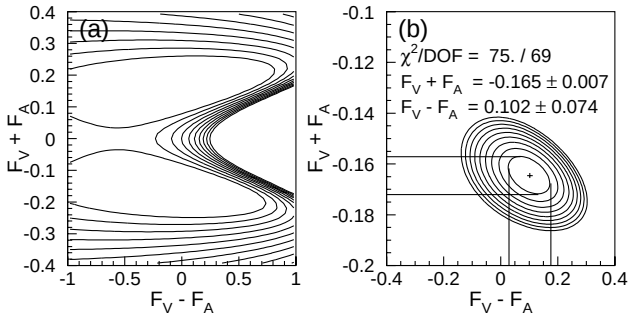

FIG. 3. χ^2 contours for the fit to the E_{μ^+} vs E_γ distribution. (a) Contours for all plausible values of the form factors. Each contour represents 50 units of χ^2. (b) Near a χ^2 minimum. In this plot, each contour corresponds to one unit of χ^2. The 1-standard-deviation uncertainties for $F_V + F_A$ and $F_V - F_A$ are also shown.

totaling 0.0007 for $|F_V + F_A|$ and 0.0097 for $F_V - F_A$. Even a much enhanced background level would have only a small effect on the measurements. Adding the individual errors in quadrature, we find a total systematic error of 0.011 for $|F_V + F_A|$ and 0.044 for $F_V - F_A$.

As a check on possible systematic errors, the branching ratio for the IB component has also been extracted. This was accomplished by normalizing to a sample of $K_{\mu 2}$ decays that was taken simultaneously with the $K_{\mu\nu\gamma}$ data. For $E_\mu > 100$ MeV and $E_\gamma > 20$ MeV, we find $B(\mathrm{IB}) = (3.6 \pm 0.3) \times 10^{-4}$, in good agreement with the theoretical value for this kinematic region, 3.3×10^{-4}. Other checks included changing the binning of the E_{μ^+} vs E_γ histogram and varying the E_γ cut. While both of these checks were limited by statistics, neither showed a systematic trend as the parameters were varied. Therefore, no systematic error is associated with these effects.

As mentioned above, the form factors F_V and F_A have, to this point, been considered independent of q^2. To assess the effect of including q^2 dependence, we assume the following form factor form:

$$F_V = \frac{F_V(q^2 = 0)}{1 - q^2/m_V^2}, \qquad F_A = \frac{F_A(q^2 = 0)}{1 - q^2/m_A^2}. \qquad (10)$$

We take $m_V = 0.870$ GeV (the K^* mass) and $m_A = 1.270$ GeV (the K_1 mass) and refit the measured $K_{\mu\nu\gamma}$ Dalitz plot in terms of the parameters $F_V(0) + F_A(0)$ and $F_V(0) - F_A(0)$. The best fit parameters are $|F_V(0) + F_A(0)| = 0.155 \pm 0.008$, $F_V(0) - F_A(0) = 0.062 \pm 0.078$. The corresponding SD^+ branching ratio is $(1.37 \pm 0.12) \times 10^{-5}$. Although the value of $|F_V(0) + F_A(0)|$ differs somewhat from that obtained assuming q^2 independence, the associated branching ratio changes only slightly. Furthermore, the minimum χ^2 of the fit is very insensitive to m_V and m_A, so we are unable to measure them and cannot offer evidence of q^2 dependence.

In conclusion, we have observed a structure-dependent component in the decay $K^+ \to \mu^+ \nu_\mu \gamma$. Under the assumption of q^2 independence, the associated form factors are $|F_V + F_A| = 0.165 \pm 0.007 \pm 0.011$, $F_V - F_A = 0.102 \pm 0.073 \pm 0.044$. Since the measurement of $F_V - F_A$ is not significantly different from zero, we add statistical and systematic errors in quadrature and calculate the 90% confidence level: $-0.04 < F_V - F_A < 0.24$. The $|F_V + F_A|$ measurement is consistent with the previous result on $K^+ \to e^+ \nu\gamma$, but disagrees with the $\mathcal{O}(p^4)$ ChPT prediction by about 2 standard deviations. This is perhaps not surprising since at higher order in ChPT kaon form factors are expected to differ from those of the pion [12]. The $\mathcal{O}(p^6)$ calculation has been done for pions [13], but not yet for kaons. The limit on $F_V - F_A$ is consistent with $\mathcal{O}(p^4)$ ChPT and is significantly better than any previously obtained from kaon decay. A more detailed description of the analysis can be found in Ref. [14].

We gratefully acknowledge the dedicated effort of the technical staff supporting this experiment and of the Brookhaven AGS Department. This research was supported in part by the U.S. Department of Energy under Contracts No. DE-AC02-98CH10886, W-7405-ENG-36, and Grant No. DE-FG02-91ER40671, by the Ministry of Education, Science, Sports and Culture of Japan through the Japan-U.S. Cooperative Research Program in High Energy Physics and under the Grant-in-Aids for Scientific Research, for Encouragement of Young Scientists, and by the Natural Sciences and Engineering Research Council and the National Research Council of Canada.

*Deceased.
†Present address: High Energy Accelerator Research Organization (KEK), Tanashi-branch, Midoricho, Tanashi, Tokyo 188-8501, Japan.
‡Present address: Brookhaven National Laboratory, Upton, New York 11973.

[1] D. E. Neville, Phys. Rev. **124**, 2037 (1961); H. Namaizawa, Prog. Theor. Phys. **39**, 860 (1968); an extensive bibliography of early papers can be found in D. Yu. Bardin and S. M. Bilen'kii, Yad. Fiz. **16**, 557 (1972) [Sov. J. Nucl. Phys. **16**, 311 (1973)]; K. A. Milton and W. W. Wada, Phys. Lett. **98B**, 367 (1981).
[2] S. G. Brown and S. A. Bludman, Phys. Rev. **136**, 1160 (1964); J. N. Huang and C. Y. Lee, Phys. Rev. D **27**, 2227 (1983). See also D. Bryman, P. Depommier, and C. Leroy, Phys. Rep. **88**, 151 (1982).
[3] J. Bijnens, G. Ecker, and J. Gasser, Nucl. Phys. **B396**, 81 (1993); J. Bijnens *et al.*, in *The Second DAPHNE Physics Handbook* (Servizio documentazione dei Laboratori Nazionali, Frascati, Italy, 1995), p. 315.
[4] We use the convention of the Particle Data Group [5], where F_V and F_A are dimensionless and larger by a factor of $\sqrt{2}$ than in many theoretical papers and where a minus sign precedes the interference term, thus changing their sign.
[5] C. Caso *et al.*, Eur. Phys. J. C **3**, 1 (1998).
[6] At $\mathcal{O}(p^4)$ in ChPT, these form factors are closely related to those of $\pi^+ \to \ell^+ \nu_\ell \gamma$. Thus, the vector form factor is predicted via CVC from the π^0 lifetime to be $F_V = 0.095 \pm 0.002$ and the axial form factor from the F_A measured in $\pi^+ \to e^+ \nu_e \gamma$, $F_A = 0.043 \pm 0.006$.
[7] Y. Akiba *et al.*, Phys. Rev. D **32**, 2911 (1985).
[8] J. Heintze *et al.*, Nucl. Phys. **B149**, 365 (1979).
[9] C. H. Chen, G. Q. Geng, and C. C. Lih, Phys. Rev. D **56**, 6856 (1997); G-H. Wu and J. N. Ng, Phys. Rev. D **55**, 2806 (1997); M. Kobayashi, T-T. Lin, and Y. Okada, Prog. Theor. Phys. **95**, 361 (1996); C. Q. Geng and S. K. Lee, Phys. Rev. D **51**, 99 (1995).
[10] M. S. Atiya *et al.*, Nucl. Instrum. Methods Phys. Res., Sect. A **321**, 129 (1992); S. Adler *et al.*, Phys. Rev. Lett. **79**, 2204 (1997).
[11] The best-fit SD^+ branching ratio in the $\cos(\theta_{\mu\gamma})$ fit is $B(\mathrm{SD}^+) = (1.37 \pm 0.12) \times 10^{-5}$.
[12] L. Amettler, J. Bijnens, A. Bramon, and F. Cornet, Phys. Lett. B **303**, 140 (1993).
[13] J. Bijnens and P. Talavera, Nucl. Phys. **B489**, 387 (1997).
[14] M. R. Convery, Ph.D. thesis, Princeton University, 1996.